Mem. S.A.It. Vol. 94, 221

Memorie della

The contribution of high-z AGN to the Ionizing UV background

A. Grazian

INAF–Osservatorio Astronomico di Padova, Vicolo dell'Osservatorio 5, I-35122, Padova, Italy
e-mail: andrea.grazian@inaf.it

Received: 14-11-2022; Accepted: 09-12-2022

Abstract. One of the major challenges in observational cosmology is related to the redshift evolution of the hydrogen ionizing background in the Universe. It is a widespread opinion that hydrogen is mainly reionized at z=5-7 by primeval star-forming galaxies, with a minor role of active galactic nuclei. In order to carry out an acid test of this scenario, it is fundamental to precisely measure the photo-ionization rate produced by active SMBHs, which critically depends on two main parameters: the luminosity density and the Lyman Continuum escape fraction of ionizing photons produced by high-z AGN. Based on our recent spectroscopic campaigns at $z > 4$, the derived space density of high-z AGN and their escape fraction remain substantial, leading to an important contribution of this population to the hydrogen Reionization.

Key words. Cosmology: observations, Quasars — Catalogs — Surveys — Reionization

1. Introduction

The pioneering work by Margherita Hack on the observations of the eclipsing binary ϵ-Aurigae (Hack & Selvelli 1979) testifies her long lasting legacy, especially in the study of ultra-violet (UV) radiation. At that time, observing the Universe through UV radiation required state-of-the-art instrumentation on devoted space telescopes, e.g. the International Ultraviolet Explorer (IUE). Nowadays, astronomers working on rest-frame UV radiation of distant sources have their life much easier, since the UV radiation is redshifted to the optical/NIR bands, where it is easily accessed by ground-based instrumentation. At present, astronomers are facing with different problems, e.g. the faintness of the sources at cosmological distance, which requires big facilities, i.e. telescopes with 8-10 meter primary mirror. A notable example of these difficulties is the slow advancement in the comprehension of the Epoch of Reionization (EoR) in the last twenty years.

The EoR is a sudden phase transition, when the neutral hydrogen (HI) in the Universe becomes almost completely ionized at $z \sim 5.3$ (Eilers et al. 2018; Keating et al. 2020; Bosman et al. 2022; Zhu et al. 2022). The long search for the cosmological sources responsible for this disruptive event is still on-going, with alternate luck for the two main suspects, i.e. the star-forming galaxies (Finkelstein et al. 2019)

and the active galactic nuclei (Giallongo et al. 2019).

For more than twenty years, the mainstream approach to Reionization has been focused to demonstrate that this process started early and developed in a relatively large redshift interval ($9 < z < 20$), mainly driven by faint star-forming galaxies (Bouwens et al. 2009). The neutral hydrogen fraction, however, has been observed to rapidly drop from unity to a value of $\sim 10^{-4}$ between $z \sim 7$ and $z \sim 5$ (Fan et al. 2006; Hoag et al. 2019; Planck Collaboration et al. 2020). This rapid and late reionization process is in tension with models assuming galaxies as the only contributors to the budget of HI ionizing background. Indeed, models assuming relatively faint star-forming galaxies as the main sources of the UV background show that these galaxies tend to start the reionization process too early (Naidu et al. 2020).

Motivated by these recent evidences favoring a rapid and late hydrogen reionization process completing at $z \sim 5.2 - 5.5$ and mainly driven by rare and luminous sources, we have proposed in recent years to revitalize the study of AGN as possible drivers of cosmological Reionization (Giallongo et al. 2012, 2015, 2019; Boutsia et al. 2018, 2021; Grazian et al. 2020, 2022).

The structure of this paper is the following: in Section 2 we describe the main ingredients generally adopted in order to compute the production of ionizing photons by the AGN population. Section 3 describes the recent achievements on the luminosity function of high-z AGN and their implications on the number of HI ionizing photons. A summary is provided in Section 4.

2. Production of ionizing radiation by AGN

The main ingredients needed to calculate the HI photo-ionization rate produced by high-z AGN are their luminosity function at 1450 Å rest frame, their average spectral shape at $\lambda \leq 912$ Å rest frame and their Lyman Continuum (LyC) escape fraction. The mean free path of ionizing photons in the Inter Galactic Medium (IGM) is another crucial physical parameter. Regarding AGN, these physical properties are all measurable directly, at variance with star-forming galaxies, where they must be inferred with indirect methods. In the following, we will discuss the current knowledge of these physical parameters for the AGN population.

2.1. The spectral slope of high-z AGN

The observed LyC radiation of high-z sources is mainly affected by the IGM absorption (Inoue et al. 2014). In order to derive the ratio between ionizing (at $\lambda \sim 900$ Å rest-frame) and non-ionizing (at $\lambda \sim 1450$ Å rest-frame) radiation for AGN, e.g. $L(900)/L(1450)$, the intrinsic (i.e. corrected by IGM) spectral energy distribution (SED) of AGN has been investigated. At $\lambda \geq 1216$ Å rest-frame, corresponding to the Lyman-α emission, the SED of AGN can be well approximated by a power law. At $\lambda < 1216$ Å rest-frame the power law usually shows a break (Stevans et al. 2014). At $z \sim 2.5$, the AGN spectra have a typical slope of $\alpha_\nu \sim -1.7$ at $\lambda < 1000$ Å rest-frame Lusso et al. (2015), with $\alpha_\nu = -0.61$ at $\lambda \geq 1000$ Å rest-frame, as also shown by Cristiani et al. (2016) at $z \sim 4$. With these spectral energy distributions, the observed ratio typical of high-z AGN is $L(1450)/L(900) \sim 1.5$.

2.2. The LyC escape fraction of high-z AGN

Low-z AGN emit copious amount of HI ionizing photons (Stevans et al. 2014; Lusso et al. 2015). At $z \sim 4$, an epoch where the IGM is not yet suppressing the emergent LyC radiation, the stacking analysis of thousands of SDSS QSO at bright absolute magnitudes ($M_{1450} \leq -26$) shows that the LyC escape fraction is substantial, i.e. of the order of 70-100% (Prochaska et al. 2009; Worseck et al. 2014; Cristiani et al. 2016; Romano et al. 2019).

The same measurements at fainter luminosities are not trivial. In order to carry out such measurements, very deep spectra in the UV wavelengths are needed. Current facilities (e.g. FORS at VLT and MODS at LBT, see Fig.

1) are required in order to reach those depths, as discussed in Grazian et al. (2018) and in Romano et al. (2019). The resulting LyC escape fraction of $M_{1450} \leq -24$ AGN at $z \leq 4$ is above 70% (Grazian et al. 2018) and it does not depend on the AGN luminosities. There are however opposite results from a sample of faint AGN at $3.3 < z < 4$ observed by Iwata et al. (2022) in narrow band filters covering the LyC radiation. It is worth stressing here that narrow band filters are not optimal for disentangling a low LyC escape fraction from the effect of an intervening Lyman limit system suppressing the flux at wavelengths slightly larger than the narrow band filter, as discussed in Romano et al. (2019).

3. The luminosity function of high-z AGN

Recent surveys of AGN at $z \sim 3-5$ have confirmed that the AGN luminosity function has a relatively steep faint-end slope (Glikman et al. 2010; Boutsia et al. 2018; Giallongo et al. 2019; Grazian et al. 2020), with a large space density of active SMBHs at $L \sim 0.1-1L^*$. A number of criticisms have been raised against this picture by e.g. Matsuoka et al. (2018); McGreer et al. (2018); Kulkarni et al. (2019); Niida et al. (2020); Kim et al. (2020); Jiang et al. (2022); Shin et al. (2022).

Using spectroscopically confirmed QSO samples in wide and relatively deep area from the QUBRICS and HSC surveys, Grazian et al. (2022) and Grazian et al. in prep. have shown that the previous determinations of the bright end of the QSO Luminosity Function at $z \sim 5$ are significantly underestimated by a factor of $\sim 2-3$, as shown in Fig. 2. Recent preliminary results by the CEERS survey seem to indicate that the space density of $z \sim 5$ AGN at $M_{1450} \sim -19.5$ is relatively high (Onoue et al. 2022), confirming the early determinations by Giallongo et al. (2019); Grazian et al. (2020).

3.1. The photo-ionization rate produced by $z > 4$ AGN

A recent assessment of the HI photo-ionization rate produced by $z \sim 4$ AGN has been provided by Boutsia et al. (2021). The combination of the wide surveys, e.g. QUBRICS (Calderone et al. 2019; Boutsia et al. 2020; Guarneri et al. 2021) with deep observations (Fontanot et al. 2007; Glikman et al. 2011; Boutsia et al. 2018; Giallongo et al. 2019) allows to constrain with high accuracy both the shape and the normalization of the AGN luminosity function at $z \sim 4$ in a wide luminosity range, i.e. $-30 \leq M_{1450} \leq -18$ (Boutsia et al. 2021). The mean escape fraction for the QSO and AGN population is $\sim 70\%$ (Cristiani et al. 2016; Grazian et al. 2018; Romano et al. 2019), while the mean free path of ionizing photons is 41.3 proper Mpc at z = 3.9 (Prochaska et al. 2009; Worseck et al. 2014). Adopting these ingredients, and extending them in the luminosity range $-30 \leq M_{1450} \leq -18$, Boutsia et al. (2021) concluded that AGN can produce $\sim 100\%$ of the HI ionizing background at $z \sim 4$, measured in the IGM through Lyman forest fitting or via Proximity effect. The crucial parameter entering in this calculation is the number density of faint AGN ($M_{1450} \geq -24$) at high-z, where the few available results at present are affected by large scatter, as shown in Fig. 2.

At $z \sim 5$, Grazian et al. (2022) find that the redshift evolution of the AGN luminosity function is milder than previously reported determinations, e.g. from SDSS survey. As a consequence, the $z \sim 5$ AGN luminosity function shows a shape similar to the one derived with greater accuracy at $z \sim 4$ adopting a slightly lower normalization, by ~ 0.25 dex. Adopting an escape fraction of $\sim 70\%$ and a mean free path of 17.4 proper Mpc at $z = 4.75$ from Worseck et al. (2014), the derived photo-ionization rate in Grazian et al. (2022) is ~50-100% of the UV background (UVB) needed to keep the IGM highly ionized just at the end of the reionization epoch, supporting a scenario where AGN can play an important role in the cosmological reionization process.

4. Summary

Recent surveys based on deep and wide imaging databases, artificial intelligence tools to select their candidates, and massive

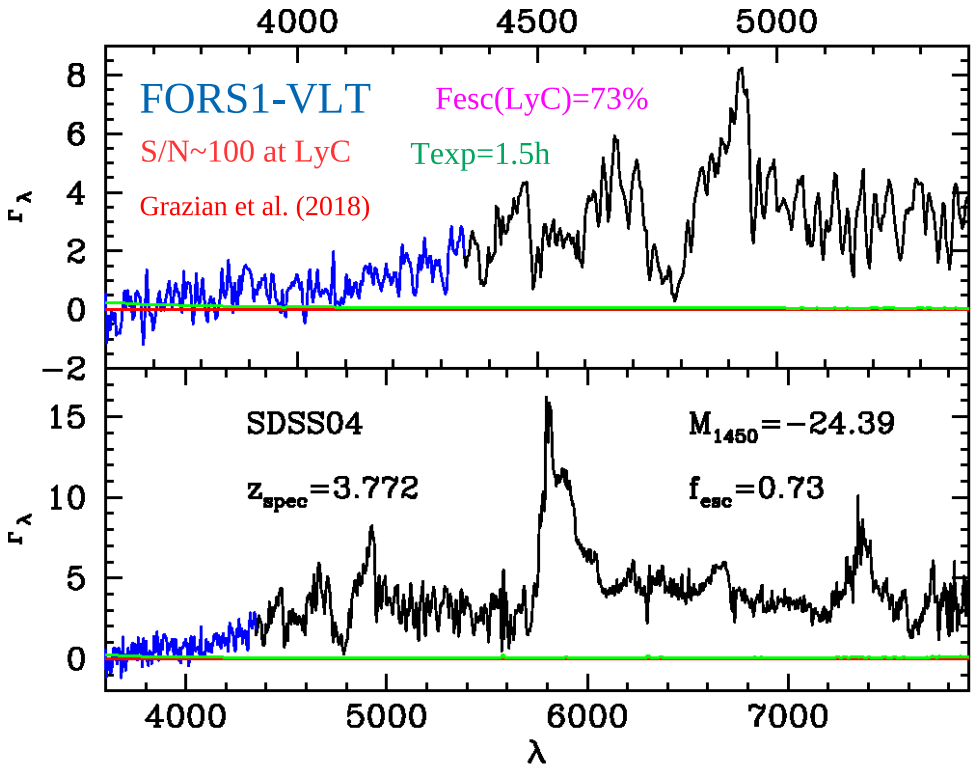

Fig. 1. The detection of the LyC emission by a relatively faint ($M_{1450} \sim -24.4$) AGN at $z \sim 4$ observed with FORS instrument at VLT with the blue enhanced detectors. Image adapted from Grazian et al. (2018).

spectroscopic identification, e.g. QUBRICS (Calderone et al. 2019; Boutsia et al. 2020; Guarneri et al. 2021), are changing our comprehension of the Epoch of Reionization. Thanks to these efforts, a number of new achievements have been reached in the last few years:

- The LyC escape fraction of bright ($M_{1450} \sim -27$) AGN at $z > 4$ is substantial, of the order of ~70% (Cristiani et al. 2016). No evolution of the LyC escape fraction with AGN luminosity has been detected (Grazian et al. 2018).
- The space density of bright QSOs and faint AGN is relatively high both at $z \sim 4$ (Boutsia et al. 2018, 2021) and at $z \sim 5$ (Giallongo et al. 2019; Grazian et al. 2020, 2022).
- The bright end of the QSO Luminosity Function at $z > 4$ is ~2-3 times higher than previous determinations (Boutsia et al. 2021; Grazian et al. 2022).
- At $z \sim 4-5$ AGN produce ~50-100% of HI ionizing background (Boutsia et al. 2021; Grazian et al. 2022). AGN could thus be the main producers of HI ionizing background at $z > 4$.

In summary, our recent results are supporting an increasingly important role of AGN as ionizing sources in the Epoch of Reionization. JWST will provide crucial information in this context.

Acknowledgements. AG warmly thanks the Organizers of the Hack100 Conference for the very interesting and stimulating meeting.

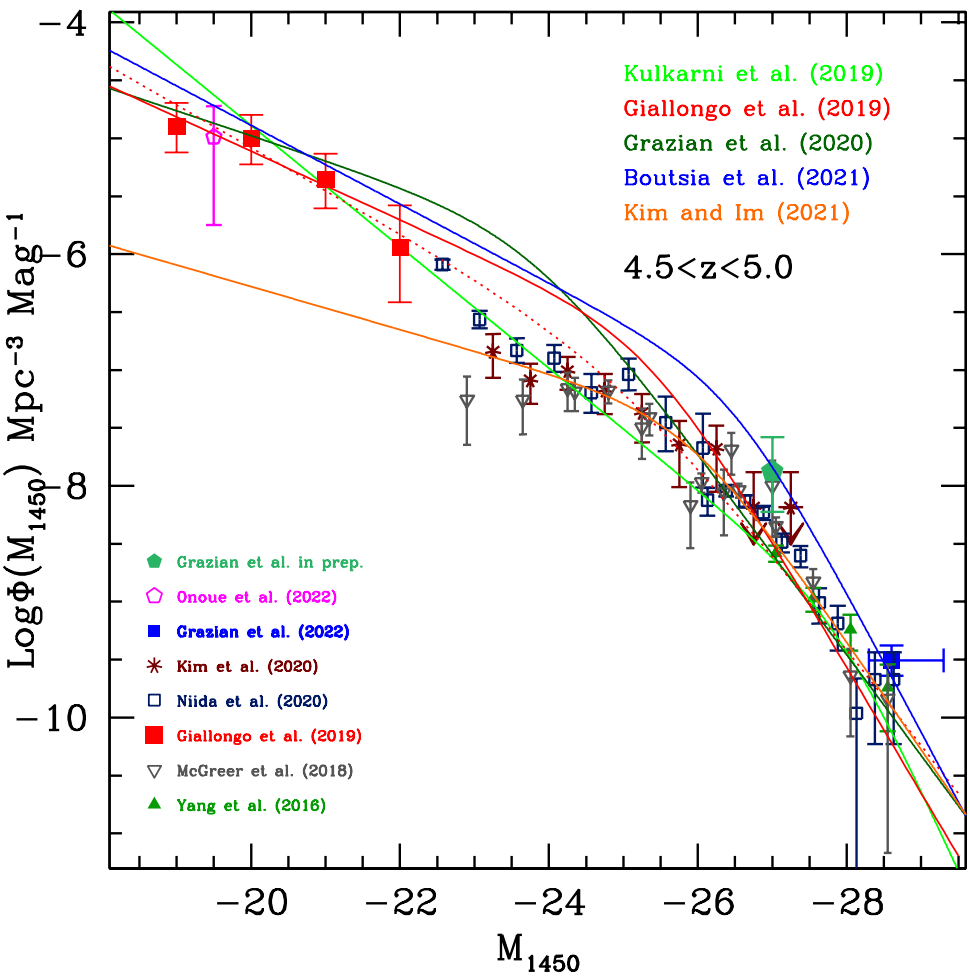

Fig. 2. The QSO Luminosity Function at $z \sim 5$ from recent surveys. The filled blue square and green pentagon by Grazian et al. (2022) and Grazian et al. in prep., respectively, are indicating that previous determinations of the QSO space density at bright and intermediate absolute magnitudes were significantly underestimated. The blue line shows the luminosity function of Boutsia et al. (2021), corrected in space density with the redshift evolution found by Grazian et al. (2022). The open magenta pentagon at $M_{1450} \sim -19.5$ shows the QSO luminosity function of Onoue et al. (2022) from JWST, with the error bars adapted from the Gehrels (1986) statistics, which is valid for low number counts.

References

Bosman, S. E. I., Davies, F. B., Becker, G. D., et al. 2022, MNRAS, 514, 55

Boutsia, K., Grazian, A., Calderone, G., et al. 2020, ApJS, 250, 26

Boutsia, K., Grazian, A., Fontanot, F., et al. 2021, ApJ, 912, 111

Boutsia, K., Grazian, A., Giallongo, E., Fiore, F., & Civano, F. 2018, ApJ, 869, 20

Bouwens, R. J., Illingworth, G. D., Franx, M.,

et al. 2009, ApJ, 705, 936
Calderone, G., Boutsia, K., Cristiani, S., et al. 2019, ApJ, 887, 268
Cristiani, S., Serrano, L. M., Fontanot, F., Vanzella, E., & Monaco, P. 2016, MNRAS, 462, 2478
Eilers, A.-C., Davies, F. B., & Hennawi, J. F. 2018, ApJ, 864, 53
Fan, X., Carilli, C. L., & Keating, B. 2006, ARA&A, 44, 415
Finkelstein, S. L., D'Aloisio, A., Paardekooper, J.-P., et al. 2019, ApJ, 879, 36
Fontanot, F., Cristiani, S., Monaco, P., et al. 2007, A&A, 461, 39
Gehrels, N. 1986, ApJ, 303, 336
Giallongo, E., Grazian, A., Fiore, F., et al. 2015, A&A, 578, A83
Giallongo, E., Grazian, A., Fiore, F., et al. 2019, ApJ, 884, 19
Giallongo, E., Menci, N., Fiore, F., et al. 2012, ApJ, 755, 124
Glikman, E., Bogosavljević, M., Djorgovski, S. G., et al. 2010, ApJ, 710, 1498
Glikman, E., Djorgovski, S. G., Stern, D., et al. 2011, ApJ, 728, L26
Grazian, A., Giallongo, E., Boutsia, K., et al. 2022, ApJ, 924, 62
Grazian, A., Giallongo, E., Boutsia, K., et al. 2018, A&A, 613, A44
Grazian, A., Giallongo, E., Fiore, F., et al. 2020, ApJ, 897, 94
Guarneri, F., Calderone, G., Cristiani, S., et al. 2021, MNRAS, 506, 2471
Hack, M. & Selvelli, P. L. 1979, A&A, 75, 316
Hoag, A., Bradač, M., Huang, K., et al. 2019, ApJ, 878, 12
Inoue, A. K., Shimizu, I., Iwata, I., & Tanaka, M. 2014, MNRAS, 442, 1805
Iwata, I., Sawicki, M., Inoue, A. K., et al. 2022, MNRAS, 509, 1820
Jiang, L., Ning, Y., Fan, X., et al. 2022, Nature Astronomy, 6, 850
Keating, L. C., Weinberger, L. H., Kulkarni, G., et al. 2020, MNRAS, 491, 1736
Kim, Y., Im, M., Jeon, Y., et al. 2020, ApJ, 904, 111
Kulkarni, G., Worseck, G., & Hennawi, J. F. 2019, MNRAS, 488, 1035
Lusso, E., Worseck, G., Hennawi, J. F., et al. 2015, MNRAS, 449, 4204
Matsuoka, Y., Strauss, M. A., Kashikawa, N., et al. 2018, ApJ, 869, 150
McGreer, I. D., Fan, X., Jiang, L., & Cai, Z. 2018, AJ, 155, 131
Naidu, R. P., Tacchella, S., Mason, C. A., et al. 2020, ApJ, 892, 109
Niida, M., Nagao, T., Ikeda, H., et al. 2020, ApJ, 904, 89
Onoue, M., Inayoshi, K., Ding, X., et al. 2022, arXiv e-prints, arXiv:2209.07325
Planck Collaboration, Aghanim, N., Akrami, Y., et al. 2020, A&A, 641, A6
Prochaska, J. X., Worseck, G., & O'Meara, J. M. 2009, ApJ, 705, L113
Romano, M., Grazian, A., Giallongo, E., et al. 2019, A&A, 632, A45
Shin, S., Im, M., & Kim, Y. 2022, ApJ, 937, 32
Stevans, M. L., Shull, J. M., Danforth, C. W., & Tilton, E. M. 2014, ApJ, 794, 75
Worseck, G., Prochaska, J. X., O'Meara, J. M., et al. 2014, MNRAS, 445, 1745
Zhu, Y., Becker, G. D., Bosman, S. E. I., et al. 2022, ApJ, 932, 76